Biogeosciences

Sedimentological processes and environmental variability at Lake Ohrid (Macedonia, Albania) between 637 ka and the present

Alexander Francke[1], Bernd Wagner[1], Janna Just[1], Niklas Leicher[1], Raphael Gromig[1], Henrike Baumgarten[2], Hendrik Vogel[3], Jack H. Lacey[4,5], Laura Sadori[6], Thomas Wonik[2], Melanie J. Leng[4,5], Giovanni Zanchetta[7], Roberto Sulpizio[8,9], and Biagio Giaccio[10]

[1]Institute of Geology and Mineralogy, University of Cologne, Cologne, Germany
[2]Leibniz Institute for Applied Geophysics (LIAG), Hannover, Germany
[3]Institute of Geological Sciences & Oeschger Centre for Climate Change Research, University of Bern, Bern, Switzerland
[4]Centre for Environmental Geochemistry, School of Geography, University of Nottingham, Nottingham, UK
[5]NERC Isotope Geosciences Facilities, British Geological Survey, Keyworth, Nottingham, UK
[6]Dipartimento di Biologia Ambientale, Università di Roma "La Sapienza", Rome, Italy
[7]Dipartimento di Scienze della Terra, University of Pisa, Pisa, Italy
[8]Dipartimento di Scienze della Terra e Geoambientali, University of Bari, Bari, Italy
[9]Istituto per la Dinamica dei Processi Ambientali (IDPA) CNR, Milan, Italy
[10]Istituto di Geologia Ambientale e Geoingegneria – CNR, Rome, Italy

Correspondence to: Alexander Francke (alexander.francke@uni-koeln.de)

Abstract. Lake Ohrid (Macedonia, Albania) is thought to be more than 1.2 million years old and host more than 300 endemic species. As a target of the International Continental scientific Drilling Program (ICDP), a successful deep drilling campaign was carried out within the scope of the Scientific Collaboration on Past Speciation Conditions in Lake Ohrid (SCOPSCO) project in 2013. Here, we present lithological, sedimentological, and (bio-)geochemical data from the upper 247.8 m composite depth of the overall 569 m long DEEP site sediment succession from the central part of the lake. According to an age model, which is based on 11 tephra layers (first-order tie points) and on tuning of bio-geochemical proxy data to orbital parameters (second-order tie points), the analyzed sediment sequence covers the last 637 kyr.

The DEEP site sediment succession consists of hemipelagic sediments, which are interspersed by several tephra layers and infrequent, thin (< 5 cm) mass wasting deposits. The hemipelagic sediments can be classified into three different lithotypes. Lithotype 1 and 2 deposits comprise calcareous and slightly calcareous silty clay and are predominantly attributed to interglacial periods with high primary productivity in the lake during summer and reduced mixing during winter. The data suggest that high ion and nutrient concentrations in the lake water promoted calcite precipitation and diatom growth in the epilimnion during MIS15, 13, and 5. Following a strong primary productivity, highest interglacial temperatures can be reported for marine isotope stages (MIS) 11 and 5, whereas MIS15, 13, 9, and 7 were comparably cooler. Lithotype 3 deposits consist of clastic, silty clayey material and predominantly represent glacial periods with low primary productivity during summer and longer and intensified mixing during winter. The data imply that the most severe glacial conditions at Lake Ohrid persisted during MIS16, 12, 10, and 6, whereas somewhat warmer temperatures can be inferred for MIS14, 8, 4, and 2. Interglacial-like conditions occurred during parts of MIS14 and 8.

1 Introduction

In the light of recent climate warming, it has become fundamentally important to understand the characteristics and shaping of individual glacial and interglacial periods dur-

ing the Quaternary, as these differences can reveal information about external forcing and internal feedback mechanisms in the global climatic system (Lang and Wolff, 2011). The global glacial–interglacial variability has widely been studied on ice cores (e.g., EPICA-members, 2004; NGRIP-members, 2004) and on marine sediment successions (e.g., Lisiecki and Raymo, 2005). In terrestrial realms, long continuous paleoclimatic records are sparse and mostly restricted to loess–paleosol sequences (e.g., Chen et al., 1999), to speleothem records (Bar-Matthews and Ayalon, 2004; Wang et al., 2008), and to lacustrine sediments (e.g., Prokopenko et al., 2006; Melles et al., 2012). In the eastern and southeastern Mediterranean region, long terrestrial paleo-records have become available from Lake Van (Stockhecke et al., 2014a), the Dead Sea (Stein et al., 2011), and from the Soreq Cave speleothem record (Bar-Matthews and Ayalon, 2004).

In the central Mediterranean region, the only terrestrial paleo-record that continuously covers more than 1 million years is the Tenaghi Philippon pollen record in northern Greece (cf. Fig. 1), which spans the last 1.3 million years and provides valuable insights into the vegetation history of the area (e.g., Tzedakis et al., 2006; Pross et al., 2015). The results from Tenaghi Philippon reveal that individual interglacial and glacial periods in the Mediterranean region can differ significantly in their duration and severity (e.g., Tzedakis et al., 2006; Fletcher et al., 2013). However, analytical methods for paleoclimate reconstructions at Tenaghi Philippon have so far been restricted to pollen analyses.

Lake Ohrid on the Balkan Peninsula is thought to be more than 1.2 million years old and has already demonstrated its high sensitivity to environmental change and the potential to provide high-resolution paleoenvironmental information for the last glacial–interglacial cycle (e.g., Wagner et al., 2008, 2009, 2014; Vogel et al., 2010a). Given that Lake Ohrid is also a hotspot for endemism with more than 300 endemic species in the lake (Föller et al., 2015), its sediments also have the potential to address evolutionary questions such as what the main triggers of speciation events are.

An ICDP deep drilling campaign took place at Lake Ohrid in spring 2013 using the Deep Lake Drilling System (DLDS) operated by the Drilling, Observation and Sampling of the Earths Continental Crust (DOSECC) consortium. More than 2100 m of sediments were recovered from four different drill sites (Fig. 1). The processing of the cores from the DEEP site from the central part of Lake Ohrid is still ongoing at the University of Cologne (Germany). Here, we present lithological, sedimentological, and (bio-)geochemical results from the upper part of the DEEP site sediment succession until 247.8 mcd (meter composite depth). According to an age model, which is based on 11 tephrochronological tie points and on tuning of bio-geochemical proxy data against orbital parameters, the analyzed sequence covers the period since 637 ka. Here, we aim to provide a chronological framework for the deposits, confirm the completeness of the record, provide first insights into the sedimentological, paleoenviron-

mental and paleoclimatological history of Lake Ohrid, and form the basis of more detailed work in the future. Furthermore, our results enable a first characterization of glacial and interglacial severity since marine isotope stage (MIS) 16.

2 Site information

Lake Ohrid is located at the border of the Former Yugoslav Republic of Macedonia (FYROM) and Albania at an altitude of 693 m above sea level (m a.s.l., Fig. 1a). The lake is approximately 30 km long, 15 km wide, and covers a surface area of 358 km^2. Due to its location in a tectonic, N–S trending graben system, the lake basin is tub-shaped with a mean water depth of 150 m and a maximum water depth of 293 m (Fig. 1b). The water volume calculates to 55.4 km^3. The lake is mainly fed by karstic inflow (55 %, e.g., Matzinger et al., 2007; Vogel et al., 2010a) and by small rivers. The karstic inflow partly originates from Lake Prespa, located at an altitude of 848 m a.s.l. ca. 10 km to the east of Lake Ohrid (Fig. 1b). Both lakes are connected via karstic aquifers. The lake level of Ohrid is balanced by a surface outflow in the northern corner (Crim Drim River, 60 %, Fig. 1b), and by evaporation (40 %, Matzinger et al., 2006b). The large water volume and the high proportion of karstic inflow induce an oligotrophic state in Lake Ohrid. A complete overturn of the water column occurs approximately every 7 years (e.g., Matzinger et al., 2007), although the upper approximately 200 m of the water column are mixed every year.

The catchment of Lake Ohrid comprises 2393 km^2 including Lake Prespa (Fig. 1b). Both lakes are separated by the Galicica mountain range that is up to 2300 m a.s.l. high (Fig. 1b). To the west of Lake Ohrid, the Mocra mountain chain rises up to about 1500 m a.s.l. The morphostructure with high mountains to the west and east of Lake Ohrid is mainly the result of a pull-apart-like opening of the basin during the late phases of the Alpine orogeny (Aliaj et al., 2001; Hoffmann et al., 2010; Lindhorst et al., 2015). Several earthquakes in the area (NEIC database, USGS) and mass wasting deposits, which occur in the lateral parts of Lake Ohrid (Reicherter et al., 2011; Lindhorst et al., 2012; Wagner et al., 2012), document the tectonic activity in the area until the present day.

The oldest bedrock in the catchment of Lake Ohrid is of Devonian age, consists of metasedimentary rocks (phyllites), and occurs in the northeastern part of the basin. Triassic carbonate and siliciclastic rocks occur in the southeast, east, and northwest (e.g., Wagner et al., 2009; Hoffmann et al., 2010; Vogel et al., 2010b). Ultramafic metamorphic and magmatic rocks including ophiolites of Jurassic and Cretaceous age crop out in the west (Hoffmann et al., 2010). Quaternary lacustrine and fluvial deposits cover the plains to the north and to the south of Lake Ohrid (Hoffmann et al., 2010; Vogel et al., 2010b).
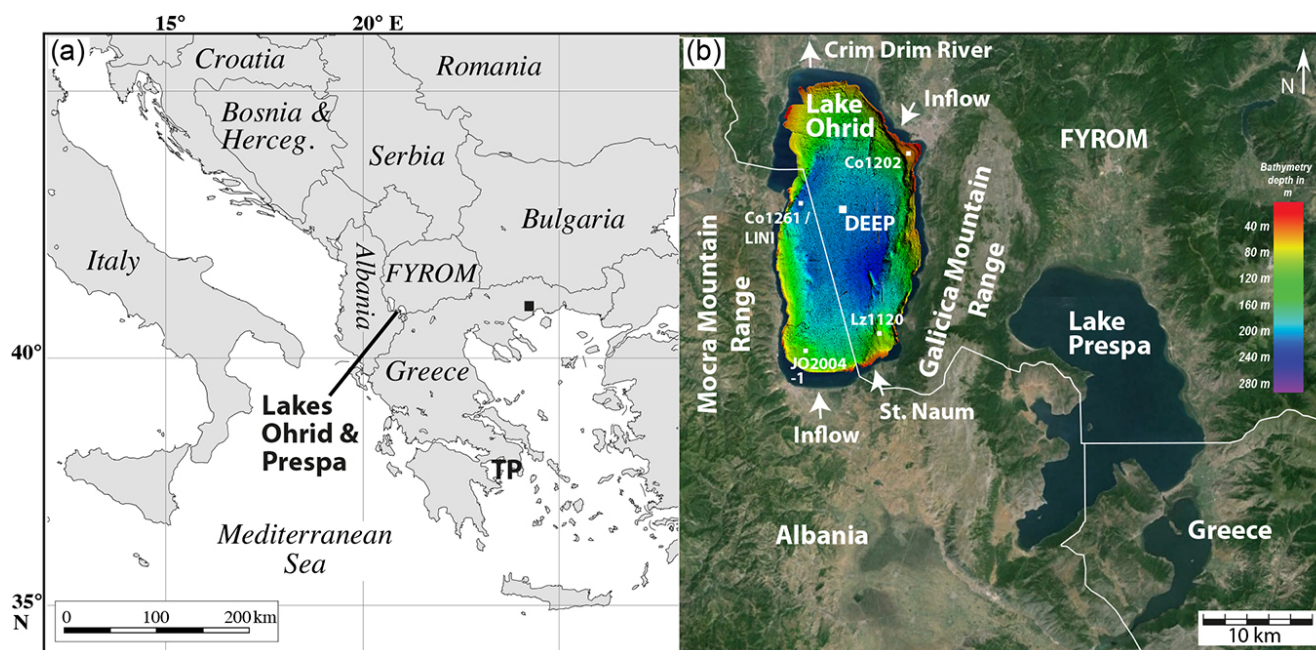
Figure 1. (a) Location of lakes Ohrid and Prespa on the Balkan Peninsula at the border of the Former Yugoslav Republic of Macedonia (FYROM) and Albania. TP: coring location of the Tenaghi Pilippon record. **(b)** Map of the area of lakes Ohrid and Prespa and bathymetric map of Lake Ohrid (from Lindhorst et al., 2015). Marked in white are the DEEP site and the short cores Lz1120 (Wagner et al., 2009), Co1202 (Vogel et al., 2010a), and LO2004-1 (Belmecheri et al., 2009).

The climate at Lake Ohrid is influenced both by continental and Mediterranean climate conditions (Watzin et al., 2002). Between summer and winter, monthly average air temperatures range between $+26$ and $-1\,°C$, respectively. The annual precipitation averages to ca. $750\,\mathrm{mm\,yr^{-1}}$, with drier conditions during summer, and more precipitation during winter. The prevailing wind directions are north and south and primarily controlled by the topography of the Lake Ohrid valley (summarized by Wagner et al., 2009).

3 Material and methods

3.1 Field work

The DEEP site (5045-1) is the main drill site in the central part of the lake at a water depth of 243 m (Fig. 1b; $41°02'57''$ N, $020°42'54''$ E). The uppermost sediments at the DEEP site down to 1.5 m below lake floor (b.l.f.) were recovered in 2011 using a UWITEC gravity and piston corer (core Co1261), as these drilling techniques provide a good core quality for sub-surface sediments. In 2013, more than 1500 m of sediments were recovered from six different drill holes (5045-1A to 5045-1F) at the DEEP site. The distance between each drill hole averages ca. 40 m. Holes 5045-1A and 5045-1E comprise sub-surface sediments down to ca. 2.4 and 5 m b.l.f., respectively. Holes 5045-1B and 5045-1C were drilled down to a penetration depth of 480 m b.l.f. At

hole 5045-1D, the maximum penetration of 569 m b.l.f. was reached. Spot coring down to 550 m blf was conducted in hole 5045-1F in order to fill any gaps present in the other holes (see also Wagner et al., 2014). After core recovery, the sediment cores were cut in (up to) 1 m long segments and stored in darkness at $4\,°C$.

During the drilling campaign in 2013, onsite core processing comprised smear-slide analyses of core catcher material and magnetic susceptibility measurements on the whole cores in 2 cm resolution using a Multi-Sensor Core Logger (MSCL, GEOTEK Co.) equipped with a Bartington MS2C loop sensor (see also Wagner et al., 2014). Following the field campaign, the cores were shipped to the University of Cologne for further analyses.

3.2 Laboratory work

A first correlation of the individual core segments to provide a preliminary composite profile for the DEEP site sequence was established based on the magnetic susceptibility data of the whole cores from holes 5045-1B, 5045-1C, 5045-1D, and 5045-1F. Cores incorporated into the composite profile were then split lengthwise and described for color, grain size, structure, macroscopic components, and calcite content (reaction with 10 % HCl). High-resolution line scan images were taken using the MSCL (GEOTEK Co.). X-ray fluorescence (XRF) scanning was carried out at 2.5 mm resolution and with an integration time of 10 s using an ITRAX core

Table 1. The contributions of the different core sections to the composite DEEP site profile.

Hole	Number of core runs	Number of sections
Co1261	2 (1.1 %)	2 (0.5 %)
5045-1B	26 (14.2 %)	50 (12.9 %)
5045-1C	72 (39.3 %)	137 (35.3 %)
5045-1D	75 (41.0 %)	184 (47.4 %)
5045-1F	8 (4.4 %)	15 (3.9 %)
Σ	183	388

scanner (Cox Analytical, Sweden). The ITRAX core scanner was equipped with a chromium (Cr) X-ray source and was run at 30 kV and 30 mA. Data processing was performed with the QSpec 6.5 software (Cox Analytical, Sweden; cf. Wennrich et al., 2014). In order to account for inaccuracies and to validate the quality of the XRF scanning data, conventional wavelength dispersive XRF (WDXRF, Philips PW 2400, Panalytical Cor., the Netherlands) was conducted at 2.56 m resolution. The optical and lithological information (layer by layer correlation) was then combined with XRF scanning data to fine-tune the core correlation by using the Corewall software package (Correlator 1.695 and Corelyzer 2.0.1).

If an unequivocal core correlation was not possible, additional core sections from other drill holes in the respective depths were opened, likewise analyzed, and used to refine the core correlation. In the composite profile, the field depth measurements based on "meters below lake floor" (m b.l.f.) were replaced by "meters composite depth" (mcd). The DEEP site composite profile down to 247.8 mcd comprises two sections of core Co1261 for the uppermost 0.93 mcd and a total of 386 core sections from holes 5045-1B, 5045-1C, 5045-1D, and 5045-1F (Fig. 2, Table 1). The overall recovery of the composite profile calculates to 99.97 %, as no overlapping sequences were found between core run numbers 80 and 81 in hole 5045-1C. The length of the core catcher (8.5 cm) between these two runs led to one gap between 204.719 and 204.804 mcd.

At 16 cm resolution, 2 cm thick slices (40.7 cm^3) were removed from the core half and separated into four subsamples to establish a multiproxy data set. Intermediate intervals (8 cm distance to the 2 cm thick slices) were subsampled for high-resolution studies by pushing two cylindrical plastic vials (diameter = 0.9 cm, height = 4 cm, volume = 2.5 cm^3) into the core halves. In addition, samples for paleomagnetic analyses were taken in plastic cubes (volume of 6.2 cm^3) at 50 cm resolution until 100 mcd, and at 48 cm resolution below this depth (cf. Just et al., 2015).

All sub-samples (8 cm resolution) were freeze-dried, and the water content was calculated by the difference in weight before and after drying. For every other sample, an aliquot of about 100 mg was homogenized and ground to < 63 µm.

For the measurement of total carbon (TC) and total inorganic carbon (TIC) using a DIMATOC 100 carbon analyzer (Dimatec Corp., Germany), 40 mg of this aliquot were dispersed with an ultrasonic disperser in 10 mL DI water. TC was measured as released CO_2 after combustion at 900 °C. The TIC content was determined as CO_2 after treating the dispersed material with phosphoric acid (H_3PO_4) and combustion at 160 °C. The total organic carbon (TOC) content was calculated from the difference between TC and TIC. For the measurement of total sulfur (TS) and total nitrogen (TN), 10 mg of the ground material were analyzed using an elemental analyzer (vario MICRO cube, Elementar Corp.) after combustion at 1150 °C.

Biogenic silica (bSi) concentrations were determined at 32 cm resolution by means of Fourier transform infrared spectroscopy (FTIRS) at the Institute of Geological Sciences, University of Bern, Switzerland. For sample preparation, 11 mg of each sample were mixed with 500 mg of oven-dried spectroscopic grade potassium bromide (KBr, Uvasol®, Merck Corp.) and subsequently homogenized using a mortar and pestle. A Bruker Vertex 70 equipped with a liquid nitrogen cooled MCT (mercury–cadmium–telluride) detector, a KBr beam splitter, and a HTS-XT accessory unit (multisampler) was used for the measurement. Each sample was scanned 64 times at a resolution of 4 cm^{-1} (reciprocal centimeters) for the wavenumber range from 3750 to 520 cm^{-1} in diffuse reflectance mode. After the measurements, a linear baseline correction was applied to normalize the FTIR spectra and to remove baseline shifts and tilts by setting two points of the recorded spectrum to zero (3750 and 2210–2200 cm^{-1}). The determination of bSi from FTIR spectral information relies on spectral variations in synthetic sediment mixtures with known bSi concentrations and calibration models between the FTIR spectral information and the corresponding bSi concentrations based on partial least squares regression (PLSR, Wold et al., 2001, and references therein). For details and information regarding ground truthing of the calibration, see Meyer-Jacob et al. (2014).

For grain size analyses at 64 cm resolution, 1.5 g of the sample material were treated with hydrogen peroxide (H_2O_2, 30 %), hydrochloric acid (HCl, 10 %), and sodium hydroxide (NaOH, 1M) in order to remove authigenic matter and $Na_4P_2O_7$ for sample dispersion. Prior to the analyses, the sample material was dispersed on a shaker for 12 h and underwent 1 min of ultrasonic treatment. Sample aliquots were then measured three times with a Saturn DigiSizer 5200 laser particle analyzer equipped with a Master Tech 52 multisampler (Micromeritics Co., USA) and the individual results were averaged. Data processing was carried out by using the GRADISTATv8 program (Blott and Pye, 2001).
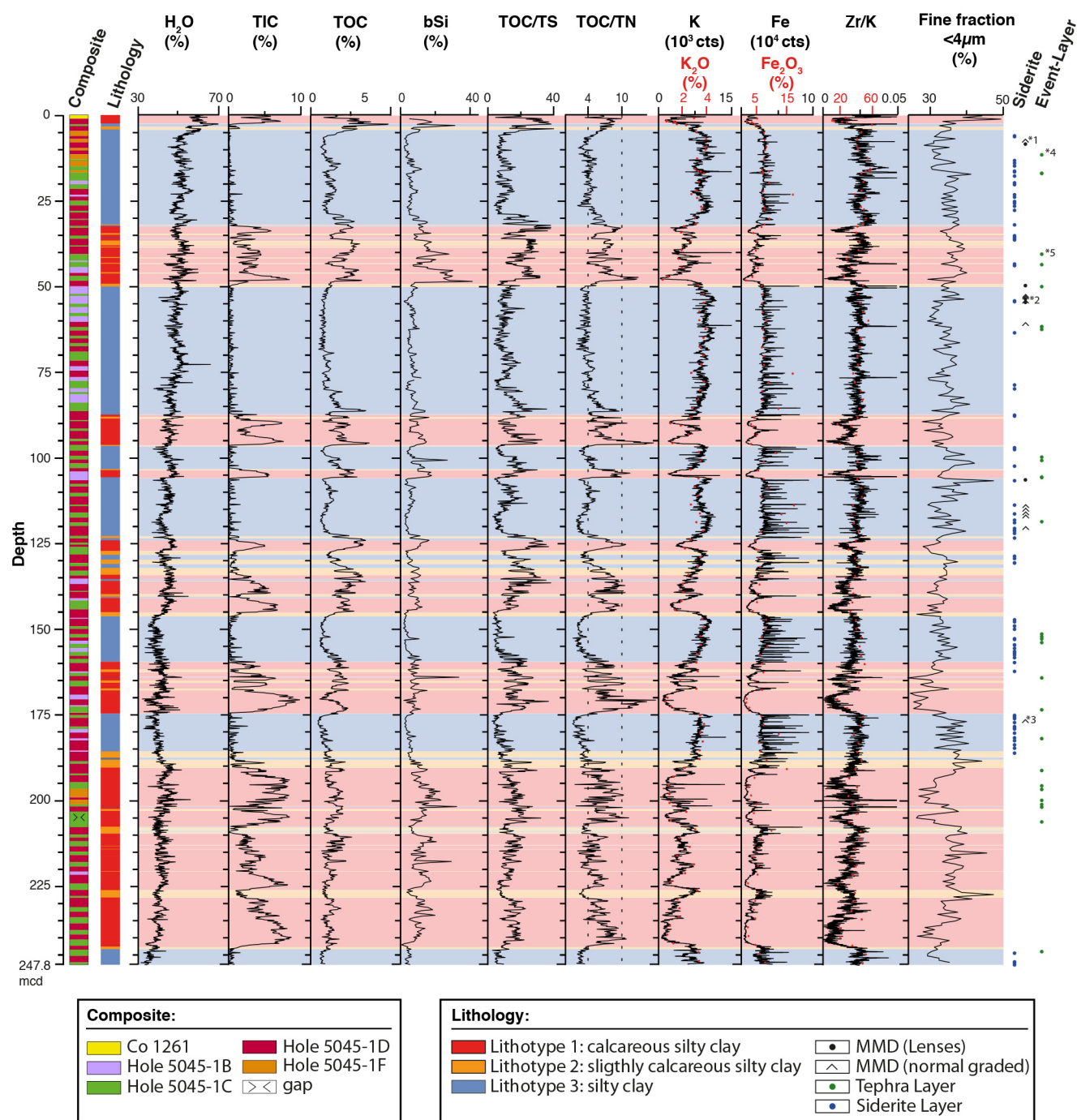
Figure 2. Variations of the lithological and (bio-)geochemical proxy data of the DEEP site sequence plotted against meter composite depth (mcd). The core composite profile of the DEEP site sediment sequence consists of core sections from core Co1261 (upper 0.93 mcd) and of core sections from holes 5045-1B, 5045-1C, 5045-1D, and 5045-1F (cf. legend "Composite"). The gap in the composite profile between 204.719 and 204.804 mcd is also marked where no overlapping core segments are available. The lithological information includes the classification of the sediments into the three lithotypes (for the color code, see legend "Lithology") and information about the water content, TIC, TOC, bSi, TOC/TS, TOC/TN, K, Fe, Zr/K, and grain size variability (< 4 µm grain size fraction). High-resolution XRF data were filtered by using a lowpass filter (fifth order, cut-off frequency 0.064 Hz) in order to remove white noise from the data. Red dots mark the results of the conventional XRF analyses. The occurrence of siderite layers, tephra layers, and mass movement deposits (MMDs) are indicated in the right column (cf. legend "Lithology"). Tephra layers and MMDs marked with an asterisk are shown in Fig. 3: *1: M; *2: O; *3: N; *4: P; *5: H.

4 Results and discussion

4.1 Lithology

The sediments from the DEEP site sequence down to 247.8 mcd consist of fine-grained hemipelagic sediments, which are sporadically interspersed by more coarse-grained event layers. From the top to the bottom of the sequence, the water content decreases from a maximum of 70 % to a minimum of 32 % due to compaction by overlying deposits (cf. Fig. 2, for detailed studies on the sediment compaction at the DEEP site, see Baumgarten et al., 2015).

4.1.1 Hemipelagic sediments

The hemipelagic deposits of the DEEP site sequence were subdivided into three lithotypes (Figs. 2 and 3) based on information from the visual core descriptions. This includes variations in the sediment color and structure.

The sediments of lithotype 1 (calcareous silty clay, Fig. 2) have very dark greenish grey to greenish grey colors, and appear massive or mottled (cf. Fig. 3a to d). Silt to gravel-sized vivianite concretions occur irregularly distributed within lithofacies 1 and can be identified by a color change from grey/white to blue after core opening.

TIC contents between 2.0 and 9.7 % imply that calcite ($CaCO_3$) is abundant in lithotype 1 sediments. Changes in color correspond to different calcite and TOC contents in the deposits (Fig. 3). The TOC content can be used as an indicator of the amount of finely dispersed organic matter (OM) in lacustrine deposits (e.g., Cohen, 2003; Stockhecke et al., 2014b). In the sediments of lithotype 1, bright colors (greenish grey) are commonly correlated with massive layers and are indicative of high calcite and low OM contents. Dark (very dark greenish grey, dark greenish grey) lithotype 1 deposits appear mottled and have lower calcite and higher OM concentrations. The bSi content varies between 1.9 and 42.5 % in the sediments of lithotype 1 and is a measure of the number of diatom frustules in the sediments of Lake Ohrid (Vogel et al., 2010a). Additional contributions to the bSi content come from sponge spicules, which were observed in smear slides. Extraordinarily high bSi concentrations of up to 42.5 % are restricted to discrete layers. Low potassium intensities (K, Fig. 2) correspond to minima in the fine fraction ($< 4 \mu m$, Fig. 2) of the grain size classes and imply a low abundance of siliciclastic minerals in the bulk sediment composition of lithotype 1 deposits (cf. Arnaud et al., 2005; Wennrich et al., 2014).

Lithotype 2 (slightly calcareous silty clay) sediments are greenish black and very dark greenish grey in color, and appear mottled or massive (cf. Fig. 3e to h). Vivianite concretions occur irregularly, and yellowish brown layers exhibit high amounts of siderite crystals in smear slides (Figs. 2 and 4). The occurrence of siderite in the DEEP site sediments was confirmed by means of XRD, EDX, and FTIRS spectroscopy (Lacey et al., 2015b).

TIC contents between 0.5 and 2 % indicate that calcite is less abundant in lithotype 2 sediments. Distinct peaks in the TIC content correspond to peaks in Fe and Mn counts and to the occurrence of the yellowish brown siderite layers (Fig. 4). The greenish black sediment successions of lithotype 2 sediments are mottled and have high amounts of OM, as indicated by TOC contents of up to 4.5 %. Brighter, very dark greenish grey sections can be massive or mottled and have lower TOC contents (Fig. 3). The number of diatom frustules is moderate to high, as inferred from bSi contents between 2 and 27.9 %. The bulk sediment composition is balanced by moderate amounts of clastic material (Fig. 2, K intensities).

The bright, greenish grey sediments of lithotype 3 (silty clay) are mottled and intercalated with massive sections of up to several decimeters in thickness (Fig. 3i to l). Vivianite concretions occur irregularly, and yellowish brown siderite layers are abundant (Fig. 2).

The TIC values of lithotype 3 sediments rarely exceed 0.5 %, which infers negligible calcite contents. Occasional peaks in TIC > 0.5 % can be attributed to the occurrence of siderite layers (Figs. 2 and 4). TOC ranges between 0.4 and 4.8 % (Fig. 2), with higher values > 2.5 % close to the lower and upper boundaries of lithotype 3 sediment sections, and between 3.21 and 2.89 mcd (Fig. 2). The amount of bSi is mostly between 1.68 and 14.5 %, except for several peaks of up to 41.3 % just above tephra layers. High potassium intensities throughout most parts of lithotype 3 sediments indicate high clastic matter contents and correspond to high percentages of the fine fraction ($< 4 \mu m$, Fig. 2).

4.1.2 Event layers

The macroscopic event layers were classified as tephra deposit if a high proportion of glass shards was observed in the smear slides, and as mass movement deposit (MMD) if predominantly coarse grains and detrital siliciclastic components occurred (cf. Figs. 2 and 3). Tephra layers in the DEEP site sequence appear as up to 15 cm thick layers and as lenses (cf. Leicher et al., 2015). Most of the tephra layers are between 0.5 cm and 5 cm thick (e.g., Fig. 3h and p). In addition, a distinct peak in the K intensities in the DEEP site sequence at 2.775 mcd was identified as the Mercato crypto tephra layer by a correlation of the K XRF curve from the DEEP site with the curve of core Co1262 (Wagner et al., 2012; for location of the core, see Fig. 1). Tephrostratigraphic investigation including geochemical and morphological analyses of glass shards enabled the correlation of 13 tephra layers from the DEEP site sequence with known volcanic eruptions or distal tephra from the central Mediterranean region (Leicher et al., 2015).

The MMDs in the DEEP site sequence are between 0.1 cm and 3 cm thick, and consist of very coarse silt to fine sand-sized material (cf. also Fig. 3m, n, and o). A higher frequency
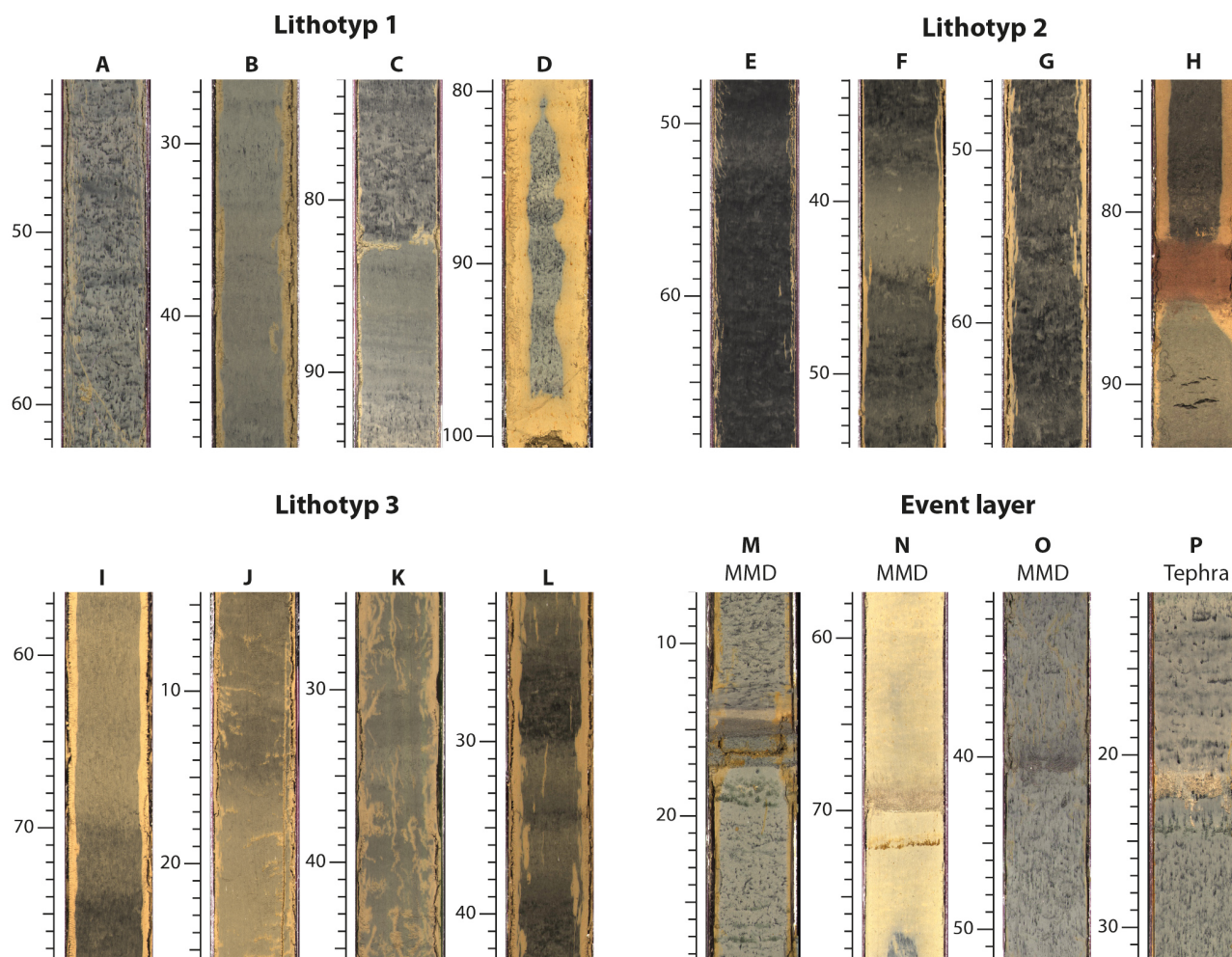
Lithotyp 1

Lithotyp 2

Lithotyp 3

Event layer

Figure 3. High-resolution line-scan images showing characteristic core segments from deposits of lithotypes 1 to 3, and of mass movement deposits (MMDs) and tephra layers. The vertical scale is in centimeter section depth. For composite depths of the line scan image, see the Supplement.

of MMDs occurs between 117 and 107 mcd, and between 55 and 50 mcd, respectively. Most of the MMDs show normal gradation (Fig. 3n) or appear as lenses (Fig. 3o). In some very thin MMDs, the gradation is only weakly expressed. The MMD in Fig. 3m differs from all other MMDs in the DEEP site sequence as it is the only one with a clay layer at the top and a 1.5 cm thick, poorly sorted, clay to fine sand-sized section at the bottom.

4.2 Sedimentary processes

4.2.1 Hemipelagic sediments

Although a detailed examination of the sediment bedding structures in the DEEP site sediments was frequently difficult due to secondary oxidation structures (cf. Fig. 3), the mottled and massive appearance and the lack of lamination imply that anoxic bottom water conditions did not occur. As massive structures commonly correspond to high calcite concentra-

tions in the sediments (high TIC), they can be explained by a high abundance of calcite crystals in the sediments.

Scanning electron microscope (SEM) and X-ray diffraction (XRD) analyses of carbonate crystals from sediment traps (Matter et al., 2010) and from sediment cores spanning the last 40 000 kyr (e.g., Wagner et al., 2009; Leng et al., 2010) show that the majority of carbonates in Lake Ohrid sediments are endogenic calcite. Only minor contributions to the calcite content come from biogenic sources; for example, from ostracod valves (Vogel et al., 2010a), detrital carbonates only occur in trace amounts (Lacey et al., 2015b). Endogenic calcite deposition in the sediments of Lake Ohrid is predominately triggered by photosynthesis-induced formation of calcite crystals in the epilimnion (e.g., Wagner et al., 2009; Vogel et al., 2010a). The precipitation occurs at warm temperatures during spring and summer, as long Ca^{2+} and HCO_3^- ions are not in short supply (e.g., Matzinger et al., 2007; Wagner et al., 2009; Vogel et al., 2010a). High Ca^{2+}
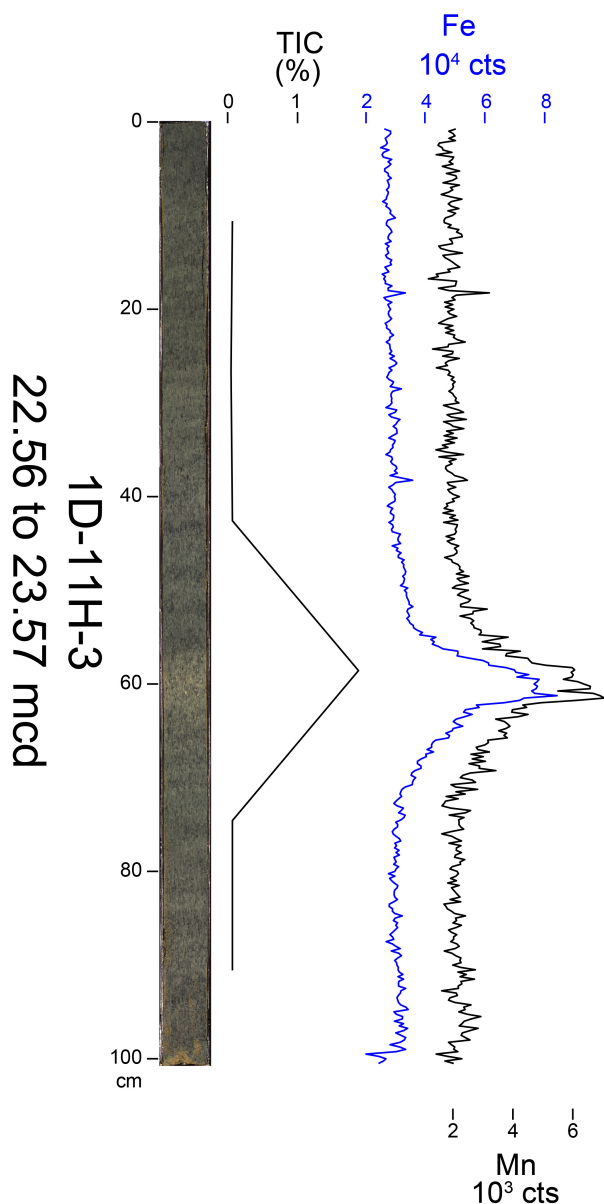
Figure 4. Siderite layer in core 1F-11H-3 (ca. 60 cm section depth) at 22.56 to 23.57 mcd. The yellowish brown siderite layer correlates with enhanced TIC, iron (Fe), and manganese (Mn) intensities in the sediments. For SEM images of the siderite, please see Lacey et al. (2015b).

and HCO_3^- concentrations in Lake Ohrid are triggered by the intensity of chemical weathering and limestone dissolution in the catchment, the karst discharge volume, and the evaporation of lake water (Vogel et al., 2010a). The calcium carbonate concentration in the sediments also depends on the preservation of the endogenic calcite. Dissolution of calcite in the lower parts of the water column, at the sediment–water interface and in the upper sediment column, can be caused by oxidation of OM, which triggers H_2CO_3 release from the surface sediments and a lowering of the lake-water pH (Müller

et al., 2006; Vogel et al., 2010a). SEM analyses of endogenic calcite in the DEEP site sediments, in addition, indicate the presence of microbial dissolution (Lacey et al., 2015b).

The high TIC contents in lithotype 1 imply high photosynthesis-induced precipitation of endogenic calcite, high temperatures during spring and summer, good calcite preservation in the sediments, and a somewhat higher lake-water pH. Lower primary productivity, lower temperatures, and a somewhat stronger dissolution of calcite can be inferred from the TIC content in lithotype 2 and 3 sediments. In lithotypes 2 and 3, siderite layers also contribute to the TIC content (cf. Figs. 2 and 4). In neighboring Lake Prespa, siderite formation has been reported to occur in the surface sediments close to the redox boundary under rather acidic and reducing conditions (Leng et al., 2013). In Lake Ohrid, DEEP site lithotype 2 and 3 sediments contain discrete horizons of authigenic siderite crystals and crystal clusters nucleating within an unconsolidated clay matrix (Lacey et al., 2015b). The open-packed nature of the matrix and growth relationships between crystals suggest that, as also observed in Lake Prespa, siderite formed in the pore spaces of the surface sediments close to the sediment–water interface, similar to other ancient lakes such as Lake Baikal (Berner, 1981; Lacey et al., 2015b).

The OM in lithotype 2 and 3 sediments is predominately of aquatic origin, as indicated by TOC / TN ratios below 10 (cf. Meyers and Ishiwatari, 1995; Wagner et al., 2009). In lithotype 1 sediments, TOC / TN occasionally exceeds 10, which could imply some contributions of terrestrial OM. However, due to the coring location in the central part of Lake Ohrid and the relatively small inlet streams, a substantial supply of allochthonous OM to the DEEP site is rather unlikely. The high TOC / TN ratios are therefore most likely a result of early digenetic selective loss of N (cf. Cohen, 2003). The aquatic origin of the OM in the sediments of the deep basin of Lake Ohrid is also in agreement with the results of Rock Eval pyrolysis from the nearby LINI drill site (Lacey et al., 2015a; see Fig. 1 for the coring location). This implies that phases characterized by higher TOC contents are representative of a somewhat elevated primary productivity. This finding is confirmed by high amounts of diatom frustules in the sediments (Wagner et al., 2009) and, accordingly, in high biogenic silica contents. Enhanced productivity in the lake requires high temperatures and sufficient nutrient supply to the epilimnion. The nutrient supply to Lake Ohrid is mainly triggered by river inflow (e.g., Matzinger et al., 2006a, b, 2007; Wagner et al., 2009; Vogel et al., 2010a), karstic inflow from Lake Prespa (Matzinger et al., 2006a; Wagner et al., 2009), and by nutrient recycling from the surface sediments (Wagner et al., 2009). Phosphorous recycling from the surface sediments is promoted by anoxic bottom water conditions and mixing can transport phosphorous from the bottom water to the epilimnion (e.g., Wagner et al., 2009). Mixing also leads to oxidation of OM at the sediment surface and, thus, to lower TOC contents. TOC preservation

in the sediments can also be modified by lake-level fluctuations, as oxidation of OM starts in the water column during settling (Cohen, 2003; Stockhecke et al., 2014b). However, distinct climate-induced lake-level fluctuations such as, for example, described for the Younger Dryas at Lake Van in Turkey (Wick et al., 2003; Stockhecke et al., 2014b, and references therein) have not been observed at Lake Ohrid in previous studies covering the last glacial–interglacial cycle (cf. Vogel et al., 2010a; Wagner et al., 2010). This can potentially be explained by the hydrological conditions at the lake, the large water volume, and the relatively high contribution of karstic groundwater inflow to the hydrological budget of Lake Ohrid. Hence, lower (higher) TOC content can be related to an overall lower (higher) productivity and/or to more (less) oxidation of OM and improved (restricted) mixing conditions.

Overall high TOC and bSi contents in lithotype 1 sediments imply high productivity as a result of high temperatures in Lake Ohrid. Less productivity and/or oxidation of OM can be inferred for sediments of lithotypes 2 and 3 from low TOC and bSi contents, and from TOC / TN ratios < 4 (cf. Leng et al., 1999). When TOC is low such as in lithotype 3 sediments, TOC / TN < 4 can be a result of OM degradation (decreasing organic C concentration) and clay-bound ammonium supply from the catchment (increasing N concentration), such as also observed in core Lz1120 from the southeastern part of the lake (Holtvoeth et al., 2015).

Good OM preservation, low oxygen availability, and overall poor mixing conditions could have favored sulfide formation in lithotype 1 sediments. Sulfide formation can be indicated by a low TOC / TS ratio (cf. Müller, 2001; Wagner et al., 2009). In lithotype 1 sediments, the high TOC / TS ratios correspond to minima in the iron intensities (cf. Fig. 2), which suggests that iron-sulfide formation was limited by iron and/or sulfate availability (cf. also Holmer and Storkholm, 2001). Sulfide formation in the sediments of Lake Ohrid is restricted to deposits where iron availability (i.e., lithotype 2 and 3 sediments) is high (cf. Just et al., 2015). Furthermore, Urban et al. (1999) have shown that early diagenetic sulfur enrichment in OM is low in oligotrophic lakes, as up to 90 % of the produced sulfides can be re-oxidized seasonally or episodically, which affects the sulfur storage over several years. At Lake Ohrid, re-oxidation of sulfides may occur during the mixing season or under present climate conditions during the irregular complete overturn of the entire water column every few years. If re-oxidation has biased the TOC / TS ratio, the lower ratios in lithotype 2 and 3 sediments are rather a result of the overall low TOC concentrations, which is confirmed by the good correspondence between the TOC / TS ratio and the TOC content.

Elemental intensities of the clastic matter, obtained from high-resolution XRF scanning, can provide information about the sedimentological composition of the deposits, and about erosional processes in the catchment. Variations in the potassium intensities (K, Fig. 2) and in the clastic matter con-

tent of DEEP site sequence sediments could primarily be a result of changing erosion in the catchment, such as it has also been reported from other lakes on the Balkan Peninsula (e.g., Francke et al., 2013). This implies that increased denudation and soil erosion could be inferred for lithotype 2 and 3 sediments, while less clastic matter supply occurs during deposition of lithotype 1 sediments. However, mutual dilution with authigenic components such as calcite, OM and diatom frustules can bias the potassium record as an indicator of denudation and clastic matter supply.

Potassium can occur in K-feldspars, micas, and clay minerals, and is mobilized particularly during chemical weathering and pedogenesis, and the residual soils in the catchment become depleted in potassium (Chen et al., 1999). In contrast to K, Zirconium (Zr) mostly occurs in the mineral zircon, which has a high density and resistance against physical and chemical weathering and is therefore commonly enriched in coarse-grained (aeolian) sediments. However, in lithotype 1 and 2 sediments, low Zr / K ratios match low percentages of the $< 4 \, \mu m$ fraction (cf. Fig. 2). This implies that coarse-grained sediments (low $< 4 \mu m$ percentages) are depleted in Zr and enriched in K at the DEEP site. Thus, the Zr / K ratio rather provides insights into the intensity of the chemical weathering in the catchment than being dependent on the physical grain size. As chemically altered minerals may be stored for hundreds and thousands of years in the catchment before they are eroded, transported, and finally deposited (cf. Dosseto et al., 2010), the Zr / K ratio does not provide information about weathering processes during the time of deposition at the DEEP site. The match of low Zr / K ratios and low percentages of the $< 4 \, \mu m$ fraction in lithotype 1 and 2 sediments imply that more coarse detrital matter, predominately consisting of K-rich clastic material from young and less chemically weathered soils, was deposited at the DEEP site. In contrast, high Zr / K ratios in lithotype 3 sediments match with high percentages of the $< 4 \, \mu m$ fraction and suggest that more fine-grained, chemically weathered, and K-depleted siliciclastics from mature soils were supplied to the lake. Deviations from the correspondence between Zr / K and the $< 4 \, \mu m$ grain size fraction can be explained by additional processes that affect the deposition of clastic matter at the DEEP site, such as the transportation energy in the inlet streams, lake-level fluctuations and the shoreline distance, and the strength of lake-internal current systems, respectively (cf. also Vogel et al., 2010b).

4.3 Event layers

Probable trigger mechanisms for MMDs have been widely discussed and encompass earthquakes, delta collapses, flooding events, over-steepening of slopes, rockfalls, and lake-level fluctuations (e.g., Cohen, 2003; Schnellmann et al., 2006; Girardclos et al., 2007; Sauerbrey et al., 2013). At Lake Ohrid, MMDs in front of the Lini Peninsula (Fig. 1)

and in the southwestern part of the lake were likely triggered by earthquakes (Lindhorst et al., 2012, 2015; Wagner et al., 2012). An earthquake might have also triggered the deposition of the MMD in Fig. 3m, which is composed of a turbidite succession and an underlying, poorly sorted debrite (after the classification of Mulder and Alexander, 2001). The disturbance generated by a debris flow can cause co-genetic turbidity currents of fine-grained material in front of and above the mass movement (Schnellmann et al., 2005; Sauerbrey et al., 2013). As the debrite–turbidite succession occurs at 7.87 mcd in hole 5045-1F, it likely corresponds to a massive slide complex north of the DEEP site (cf. the hydro-acoustic profile of Fig. 2 in Wagner et al., 2014). Density flows that enter the central part of the Lake Ohrid basin close to the DEEP site from the eastern or southern directions have not been observed in the upper parts of hydro-acoustic profiles (cf. Figs. 2 and 3 in Wagner et al., 2014). The three massive MMDs that occur in front of the Lini Peninsula to the west of the DEEP site (cf. Wagner et al., 2012) are likely not related to the debrite–turbidite succession in Fig. 3m. The underlying debrite does not occur in overlapping segments of holes 5045-1B, 5045-1C, and 5045-1D. Holes 5045-1B, 5045-1C, and 5045-1D form a N–S transect, whereas hole 5045-1F is located to the east. Due to the absence of the debrite deposits in most drill holes, the relatively low thickness in hole 5045-1F, and hydroplaning that generates a basal water layer below a debris flow (Mohrig et al., 1998; Mulder and Alexander, 2001), erosional processes at the DEEP site are likely low.

The sand lenses and normal graded MMDs (cf. Figs. 2, 3) can be classified as grain-flow deposits (after the classification of Mulder and Alexander, 2001; Sauerbrey et al., 2013) and are composed of reworked lacustrine sediments from shallow water depths or subaquatic slopes close to riverine inflows. Grain flows that enter the deep parts of the Lake Ohrid basin via the steep slopes might transform into a mesopycnal flow at the boundary of the hypolimnion (cf. also Mulder and Alexander, 2001; Juschus et al., 2009), which would have prevented erosion of the underlying sediments.

5 Core chronology

The chronology for the sediments of the DEEP site sequence down to 247.8 mcd was established by using tephrochronological information from 11 out of 13 tephra layers (cf. Table 2 and Leicher et al., 2015) and by cross-correlation with orbital parameters. The tephra layers were correlated with well-known eruptions from Italian volcanoes or central Mediterranean marker tephra by geochemical and morphological analyses of glass shards. Radiocarbon and $^{40}Ar/^{39}Ar$ ages were transferred from the reference records to the DEEP site sequence (tephrostratigraphic results of the DEEP site are provided by Leicher et al., 2015). $^{40}Ar/^{39}Ar$ ages from the literature were re-calculated by using the same flux standard

Table 2. Correlated tephra layers in the DEEP site sequence according to Leicher et al. (2015). $^{40}Ar/^{39}Ar$ ages from the literature were recalculated at 2σ confidence levels (Leicher et al., 2015).

Ohrid tephra (mcd)	Correlated eruption/tephra	Age (ka)
2.775	Mercato	8.540 ± 0.05[1]
11.507	Y-3	29.05 ± 0.37[1]
16.933	Y-5	39.6 ± 0.1[2]
40.486	POP2	102 ± 2.4[2]
43.513	X-6	109 ± 2[2]
49.947	P-11	133.5 ± 2[3]
61.726	Vico B	162 ± 6[2]
181.769	Pozzolane Rosse	457 ± 2[2]
195.566	SC5	493.1 ± 10.9[2]
201.782	A11/A12	511 ± 6[2]
206.08	Tufo di Bagni Albule	527 ± 2[2]

[1] Calibrated ^{14}C age, [2] recalculated $^{40}Ar/^{39}Ar$ ages, and [3] age for P-11 from Zanchetta et al. (2015).

in order to obtain a homogenous set of ages (see Leicher et al., 2015). The stratigraphic position and chronology of the OH-DP-0499/P-11 tephra layer at 49.947 mcd in different records from the vicinity of Lake Ohrid are discussed in detail by Zanchetta et al. (2015). Their results imply that the P-11 tephra layer has an age of 133 ± 2 ka, which was incorporated into the age–depth modeling. As the 11 tephra layers provide a robust basis for the age–depth model of the DEEP site sequence, the tephrostratigraphic information was used as first-order tie points.

The chronological information from the 11 tephra layers was also used to define cross-correlation points with orbital parameters, which were included in the age–depth model as second-order tie points. The tephra layers Y-5, X-6, P-11, and A11/12 were deposited when there are minima in the TOC content and in the TOC / TN ratio and when there is an inflection point (blue dots, Fig. 5) of increasing local summer insolation (21 June, 41° N). Thereby, the inflection points coincide with an increasing winter season length (21 September to 21 March, Fig. 5). Summer insolation and winter season length have a direct impact on the OM content and the TOC / TN ratio, as they may trigger primary productivity and decomposition. Low insolation and colder temperatures during summer reduce the primary productivity in the lake, but simultaneously, a shorter winter season would have reduced mixing in the lake, which reduces the decomposition of OM and increases TOC and TOC / TN (cf. Fig. 5, insolation and winter season length minima). A longer winter season improves the mixing, but a strong insolation during summer promotes the primary productivity in the lake, which also results in higher TOC and TOC / TN (cf. Fig. 5, insolation and winter season length maxima). Thus, low OM preservation and low TOC and TOC / TN in the sediments may occur when summer insolation strength and winter sea-
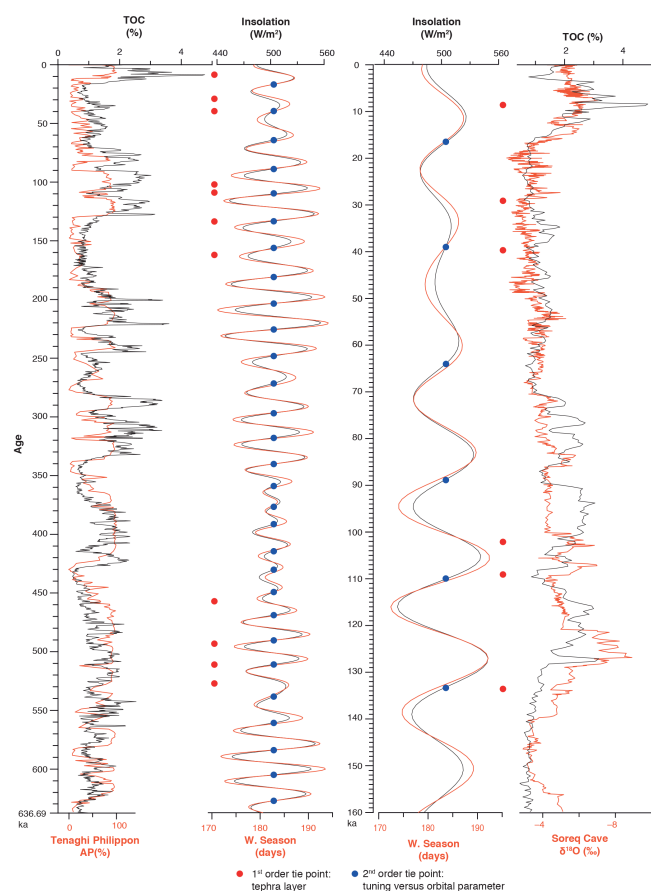
Figure 5. Left: comparison between TOC (DEEP site) and arboreal pollen percentages (AP, Tenaghi Philippon, Tzedakis et al., 2006) from 636.69 ka to the present. Right: comparison between TOC (DEEP site) and δ^{18}O (Soreq Cave, Grant et al., 2012) from 160 ka to the present. Red dots mark the tephrochonological age control points (first-order tie points); blue dots mark the TOC vs. orbital parameter tuning points (second-order tie points). The good correlation of the DEEP site TOC record with both Tenaghi Philippon and the Soreq Cave temporal series supports the age model of the DEEP site succession.

son length are balanced. In addition, the inflection points co-incide with the perihelion passage in March. As the highest proportion of the annual radiation gets lost through surface albedo during spring (Berger et al., 1981), the time period of the perihelion passage in March is characterized by cold and dry conditions in the central Mediterranean region (Magri and Tzedakis, 2000; Tzedakis et al., 2003, 2006). Cold conditions at Lake Ohrid promote mixing during winter and restrict the primary productivity during summer. Thus, minima in TOC and TOC / TN are tuned to increasing insolation and winter season length.

The 11 tephra layers and 31 cross-correlation points of second order (Supplement 1) were used for the establishment of an age–depth model. An uncertainty of ±2000 years was applied for each second-order tie point in or-

der to account for inaccuracies in the tuning process. For the age–depth modeling using the Bacon 2.2 software package (Blaauw and Christen, 2011), overall stable sedimentation rates at the DEEP site (mem.strength = 60, mem.mean = 0.9, thick = 80 cm) and expected sedimentation rates (acc.shape = 1.5, acc.mean = 20) from first age estimations for the DEEP site sequence by Wagner et al. (2014) were considered (cf. Fig. 6). Finally, the age model was evaluated and refined by a detailed comparison with the age–depth model for the downhole logging depth scale by tuning potassium counts (K) obtained from high-resolution XRF scanning to the spectral gamma radiation (SGR) of potassium (cf. Supplement 2) in hole 5045-1D (Baumgarten et al., 2015; cf. Fig. 6). The obtained age model reveals that the upper 247.8 mcd of the DEEP site sequence comprises the last ca. 637 kyr.

On the basis of the established core chronology for the DEEP site sequence, glacial–interglacial environmental variability at Lake Ohrid inferred from the TOC record is in agreement with other paleoclimate records from the Mediterranean region such as the Tenaghi Philippon (Tzedakis et al., 2006) and the Soreq Cave records (Grant et al., 2012; cf. Fig. 6). This supports the quality of the chronology for the DEEP site sediments. Whereas the chronology of the Tenaghi Philippon record is, similar to the DEEP site sequence, based on tuning against orbital parameters, the Soreq Cave speleothem record is the longest absolute dated (U-Th) paleoclimate record currently available for the Mediterranean region.

6 Overview of the paleoenvironmental history of Lake Ohrid

Variations in the TIC, bSi, TOC, K, and Zr / K records of the DEEP site sequence correspond to global and regional climatic variability on glacial–interglacial timescales, such as indicated by a comparison to the LR04 global benthic isotope stack (Lisiecki and Raymo, 2005), to the North Greenland isotope record (NGRIP-members, 2004; Barker et al., 2011), and to variations in the arboreal pollen percentage of the Tenaghi Philippon record from northern Greece (Tzedakis et al., 2006; cf. Fig. 7). In addition to the close match of climatic variability on orbital timescales between those records and the Lake Ohrid record, a comparison of the individual interglacial and glacial stages allows a first discrimination of the intensity of these stages at Lake Ohrid.

6.1 Interglacials

Between 637 ka and the present day, the DEEP site sediments deposited during the interglacial periods (MIS boundaries after Lisiecki and Raymo, 2005; see Fig. 7) mainly consist of lithotype 1 and 2 sediments. Moderate to high TIC, TOC, and bSi contents in lithotype 1 and 2 sediments imply a moderate
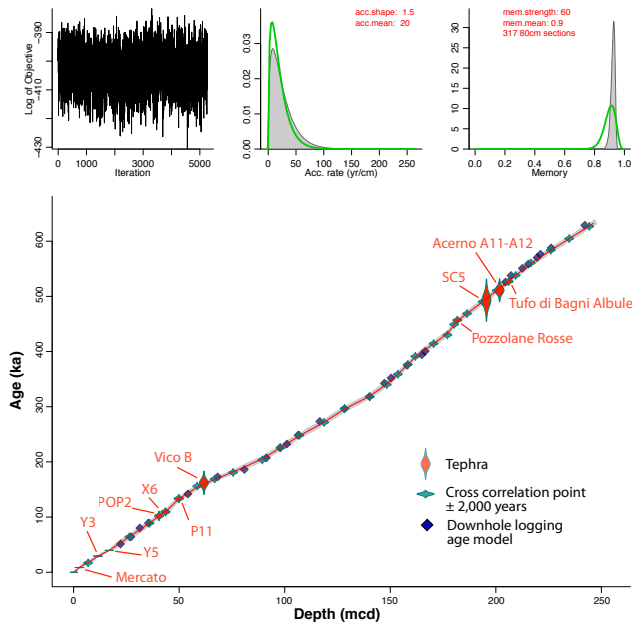
Figure 6. Age model of the DEEP site sequence down to 247.8 mcd (637 ka). Ages were calculated using the Bacon 2.2 software package (Blaauw and Christen, 2011). Overall stable sedimentation rates at the DEEP site (mem.strength = 60, mem.mean = 0.9, thick = 80 cm) and expected sedimentation rates (acc.shape = 1.5, acc.mean = 20) from first age estimations for the DEEP site sequence by Wagner et al. (2014; cf. Fig. 6) were considered. For the ages and errors of the tephra layers (red), see Table 2. The cross-correlation points (green) include an error of ±2000 years.

to strong primary productivity and, thus, moderate to high temperatures during spring and summer. The overall high temperatures during spring and summer and a longer summer season likely resulted in an incomplete and restricted mixing of the water column during winter, such it as also persists today. Poor mixing hampers the oxidative mineralization of OM and, thus, promotes the preservation of TOC and restricts the bacterial CO_2 release at the sediment surface. A reduction in the H_2CO_3 formation and a higher pH hamper the acidification in the hypolimnion and consequently improve the calcite preservation. In addition, interglacial climate conditions likely promoted high Ca^{2+} and HCO_3^- concentrations and a high pH also in the epilimnion, as warm temperatures increased chemical weathering of the limestones in the catchment. In addition, high δ^{18}O-calcite values indicating a low precipitation / evaporation (P / E) ratio (Lacey et al., 2015b), suggest that evaporation may also contribute to high Ca^{2+} and HCO_3^- concentrations in the lake water (cf. Fig. 7). Supply from the catchment and increased evaporation could have also increased the concentration of Si ions in the epilimnion, which could have promoted diatom productivity. The sensitivity of diatom productivity to increasing Si concentrations in the water column has been clearly shown in leaching experiments of tephras (D'Addabbo et al., 2015) and in high-

resolution studies of diatom changes after the deposition of the Y-5 tephra (Jovanovska et al., 2015).

Low supply of clastic matter from the catchment can be inferred for lithotype 1 and 2 sediments, where K intensities and the sedimentation rates are low ($\sim < 0.04$ cm yr^{-1}). Low supply of clastic matter is likely a result of low denudation rates despite intensive chemical weathering and pedogenesis during interglacial periods in the catchment. Relatively high pollen concentrations in the interglacial sediments of the DEEP site core imply a dense vegetation cover (cf. Fig. 7 and Sadori et al., 2015), which likely reduces erosion. In addition, the low Zr / K ratios and the low proportion of the $< 4\,\mu$m grain size fraction in lithotype 1 and 2 sediments imply that in particular K-rich minerals and the products of young soils were transported to the lake.

Lithotype 3 deposits with negligible TIC contents only occur at the onsets and terminations of interglacial periods, and during MIS7 and 3 (cf. Fig. 7). The low TIC, TOC, and bSi contents of these sediments correspond to colder periods with a restricted primary productivity. In addition, low temperatures during winter would have improved the mixing, which could promote decomposition of OM in the surface sediments and lead to lower TOC, and to lower TIC by dissolution of calcite.

6.1.1 Variations of interglacial conditions since 637 ka

Differing OM, bSi, and TIC contents in the sediments of the DEEP site sequence corresponding to interglacial time periods imply different intensities of interglacials at Lake Ohrid. Comparable conditions can be inferred for MIS15 and 13 with high TIC and bSi, and low OM, which indicate strong primary productivity and high temperatures during spring and summer, and decomposition of OM during the mixing season. However, MIS15 and 13 are regarded as relatively weak interglacials based on the synthetic Greenland isotope record (Barker et al., 2011) and the LR04 global benthic isotope stack (Lisiecki and Raymo, 2005; cf. also Fig. 7). Possible explanations could be that the inferred high intensity of these interglacials at Lake Ohrid is due to a strong seasonality or a lower water volume, which promotes a high ion concentration (high TIC, bSi) and high δ^{18}O$_{calcite}$ values in the lake water (Lacey et al., 2015b) and decomposition of OM (low TOC) during the mixing season. A lower water volume can be explained by the ongoing subsidence in the lake basin, which persists until today (Lindhorst et al., 2015).

During the first part of MIS11, between 420 and 400 ka, highest TIC concentrations along with moderate and high bSi and TOC imply highest productivity (high TOC) and highest temperatures (highest TIC), whereby the moderate bSi concentrations can be explained by mutual dilution with calcite. This is consistent with other records, where the strongest interglacial conditions and highest temperatures since 637 ka are reported for the onset of MIS11 (Lang and Wolff, 2011).
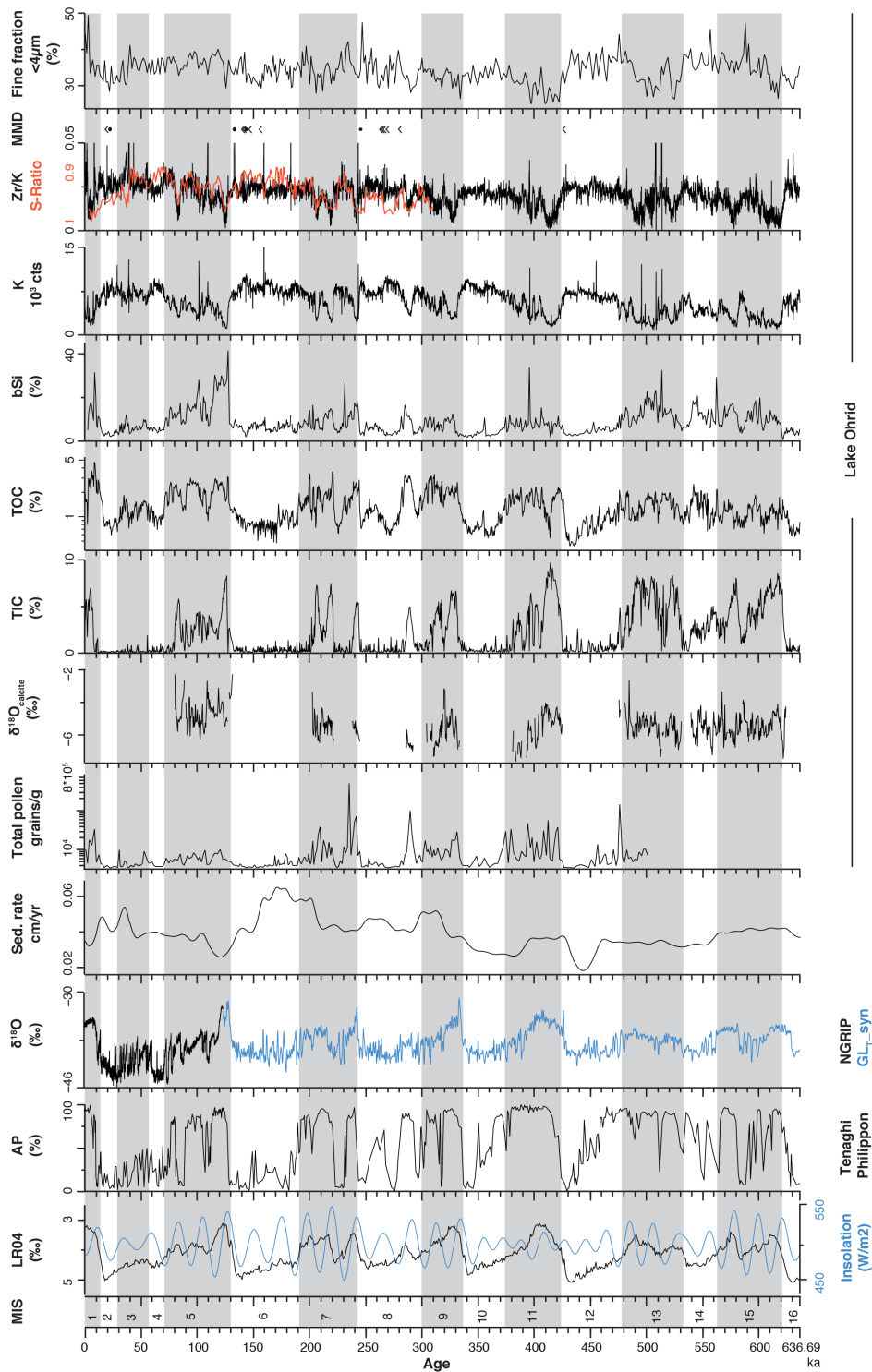
Figure 7. Proxy data from the DEEP site sediments plotted versus age and compared to the global benthic isotope stack LR04 (Lisiecki and Raymo, 2005), the local (41° N) insolation at 21 June, the arboreal pollen percentages (AP) in the Tenaghi Philippon record in northern Greece (Tzedakis et al., 2006), the North Greenland temperature derived from the NGRIP δ^{18}O record (‰ VSMOW, NGRIP-members, 2004), and the GL$_T$_syn δ^{18}O synthetic isotope record (‰ VSMOW, Barker et al., 2011). The grey shaded areas indicate interglacial marine isotope stages (MIS) according to Lisiecki and Raymo (2005). For the legend of the mass movement deposits, see Fig. 2. High-resolution XRF data and the sedimentation rate were filtered by using a lowpass filter (fifth order, cut-off frequency 0.064 Hz) in order to remove white noise from the data. Note the logarithmic scale for TOC and for the total pollen concentration. Pollen concentrations are from Sadori et al. (2015), lake water δ^{18}O$_{calcite}$ from Lacey et al. (2015b), and S-ratios representing hematite + goethite versus magnetite from Just et al. (2015).

TIC concentrations during the second phase of MIS11, between 400 and 374 ka, and during MIS9 and 7 are generally lower and mostly restricted to confined peaks, which implies overall less calcite precipitation, less primary productivity, and lower temperatures at Lake Ohrid. This is consistent with the low bSi concentrations, but not with the high TOC contents, and with relatively stronger interglacials subsequent to the MBE (Mid-Brunhes Event) inferred from the synthetic North Greenland isotope record (Barker et al., 2011) and the LR04 stack (Lisiecki and Raymo, 2005). The temperatures during the second phase of MIS11 and during MIS9 and 7 were likely lower compared to the first phase of MIS11 as indicated by the TIC record (cf. Fig. 7). In addition, the somewhat lower TIC and bSi contents also correspond to lower $\delta^{18}O_{\text{calcite}}$ in the Lake Ohrid sediments, which implies that these interglacial periods were isotopically fresher and less evaporated than the previous interglacial periods (Lacey et al., 2015b). Between 235 and 220 ka (MIS7), restricted primary productivity and improved mixing are indicated by negligible TIC and low TOC and bSi concentrations.

Overall high TIC, TOC, and bSi concentrations during MIS5 imply a strong primary productivity in the epilimnion and high temperatures during spring and summer. $\delta^{18}O_{\text{calcite}}$ during MIS5 is notably higher compared to the two previous interglacial periods (Lacey et al., 2015b) and indicates a low P / E ratio. In particular, the onset of MIS5 is reported to be one of the warmest interglacial periods in marine records (Lang and Wolff, 2011), which is also indicated in the North Greenland temperature variations (NGRIP-members, 2004; Barker et al., 2011) and in the LR04 global benthic isotope stack (Lisiecki and Raymo, 2005).

6.2 Glacials

Glacial periods between 637 ka and today are characterized by predominant deposition of lithotype 3 sediments, with rare occurrence of lithotype 1 and 2 sediments in MIS14 and 8, when TIC contents are higher. Low TOC and bSi and negligible TIC contents in lithotype 3 sediments imply low primary productivity and overall low temperatures during glacial periods. Some minor fluctuations in productivity and temperature are indicated by TOC and bSi. They are not documented in TIC, because restricted ion supply from the catchment and oxidation of OM at the sediment surface due to intensified and prolonged mixing may have led to a slight decrease in the bottom water pH and dissolution of calcite precipitated from the epilimnion. Dissolution of calcite and the existence of a threshold can also explain the delayed increase in TIC compared to TOC and bSi at the transitions of MIS16, MIS12, MIS10, MIS8, MIS6, and MIS2 into the following interglacials.

High K, a high proportion of the fine fraction $< 4\,\mu m$, and high sedimentation rates ($\sim > 0.04\,\text{cm yr}^{-1}$) despite low calcite, OM, and bSi content in the glacial sediments, indicate high input of clastic terrigenous matter and increased erosion

in the catchment. Furthermore, the high Zr / K ratios suggest the supply of K-depleted, intensively weathered siliciclastics from the catchment, which is also supported by a higher hematite + goethite to magnetite ratio (low S ratio) in glacial deposits of the DEEP site sequence (cf. Fig. 7 and Just et al., 2015). The enhanced erosion of intensively weathered siliciclastic material can be explained by less dense vegetation cover in the catchment, such as implied by low pollen concentrations in the DEEP site sequence in most of the glacial periods (cf. Fig. 7 and Sadori et al., 2015) and by the existence of local ice caps in the surrounding mountains of Lake Ohrid. The existence of ice caps is indicated by moraines in the catchment, which are thought to have formed during the last glacial cycle (Ribolini et al., 2011).

6.2.1 Variations of glacial conditions since 637 ka

As TIC is affected by dissolution, information about the severity of the individual glacials at Lake Ohrid can only be inferred from TOC and bSi. Minima in the TOC and bSi imply that most severe glacial conditions at Lake Ohrid occurred at the end of MIS16, and during MIS12, 10, and 6. Somewhat higher bSi and TOC in parts of MIS14 and 8, and in MIS6, 4, and 2, imply less severe glacial conditions. This suggests that the finding of glacial moraines from MIS2 (Ribolini et al., 2011) is probably only due to better preservation of these glacial features compared to the older glacials. Interglacial-like conditions with higher primary productivity and reduced oxidation of OM in the surface sediments prevailed at the occurrence of lithotype 1 and 2 sedimentation, i.e., between 563 and 540 ka during MIS14, and between 292 ka and 282 ka during MIS8. Interglacial-like conditions along with a forest expansion and more warm conditions between 292 and 282 ka can also be seen in the pollen records of Lake Ohrid (cf. Fig. 7 and Sadori et al., 2015) and Tenaghi Philippon (Fletcher et al., 2013).

The general observation that MIS16 and 12 were more severe glacials is in broad agreement with other records, such as the North Greenland isotope record (Barker et al., 2011), the LR04 global benthic stack (Lisiecki and Raymo, 2005), and the Tenaghi Philippon pollen record (Tzedakis et al., 2006). Thereby, the comparable low sedimentation rates in combination with the negligible TIC, bSi, and TOC concentrations between 460 and 430 ka (MIS12; cf. Fig. 7) imply low supply of clastic matter and, thus, low erosion in the catchment despite an open vegetation cover in the catchment (cf. Fig. 7 and Sadori et al., 2015). One potential explanation for the low clastic matter supply could be dry conditions and associated reductions in terrestrial runoff compared to other glacials.

The frequent occurrence of MMDs between 280 and 241 ka and between 160 and 130 ka could reflect significant lake-level fluctuations during MIS8 and 6. During the first period (MIS8), distinct fluctuations in the pollen concentrations of the DEEP site sediments (cf. Fig. 7 and Sadori et al.,

2015) correspond to similar fluctuations in the AP pollen percentages of the Tenaghi Philippon pollen record (Tzedakis et al., 2006) and probably indicate a shift from cold and dry to more warm and humid conditions in northern Greece and at Lake Ohrid. During MIS6, a 60 m lower lake level compared to present conditions and a subsequent lake-level rise during late MIS6 or during the transition from MIS6 to MIS5 are reported from hydro-acoustic and sediment core data from the northeastern corner of Lake Ohrid (Lindhorst et al., 2010). In the sediments of the DEEP site, the MIS6 to MIS5 transition occurs at ca. 50 mcd, which could indicate that the water depth might have not changed significantly compared to the present conditions. This can be explained by the ongoing subsidence (Lindhorst et al., 2015). However, the pollen record from the DEEP site also implies a phase of strong aridity during MIS6 (Sadori et al., 2015), which might imply that climate-induced lake-level fluctuations at Lake Ohrid were probably less severe compared for example to Lake Van in Turkey, where a 260 m lower lake level has been reported for the Younger Dryas (e.g., Wick et al., 2003, and references therein; Stockhecke et al., 2014b). Thereby, the extraordinarily high sedimentation rates in particular during the first part of MIS6 in combination with high K intensities and low bSi, TIC, and TOC imply intensive erosion.

7 Summary and conclusion

The investigated sediment succession between 247.8 mcd and the sediment surface from the DEEP site in the central part of Lake Ohrid provides a valuable archive of environmental and climatological change for the last 637 kyr. An age model was established by using chronological tie points from 11 tephra layers, and by tuning bio-geochemical proxy data to orbital parameters. The imprint of environmental change on the lithological, sedimentological, and (bio-)geochemistry data can be used to unravel the lake's history including the development of the Lake Ohrid basin and the climatological variability on the Balkan Peninsula.

The lithological, sedimentological, and geochemical data from the DEEP site sequence imply that Lake Ohrid did not experience major catastrophic events such as extreme lake-level low stands or desiccation events during the last 637 kyr. Hiatuses are absent and the DEEP site sequence provides an undisturbed and continuous archive of environmental and climatological change.

Based on the initial core description and the calcite content, the hemipelagic sediments from the DEEP site sequence can be classified into three different lithotypes. This classification is supported by variations in the (bio-)geochemistry proxies and matches climate variations on glacial–interglacial timescales. Overall, interglacial periods are characterized by high primary productivity during summer, restricted mixing during winter, and low erosion in the catchment. During glacial periods, the primary productivity

is low, and intense mixing of the water column promotes the decomposition of OM, which may have lowered the water pH and led to dissolution of calcite. Enhanced erosion of chemically altered siliciclastics and an overall higher clastic matter input into the lake during glacial periods can be a result of a less dense vegetation cover in the catchment and meltwater run-off from local glaciers on the surrounding mountains.

Following a strong primary productivity during spring and summer, the highest interglacial temperatures can be inferred for the first part of MIS11 and for MIS5. In contrast, somewhat lower spring and summer temperatures are observed for MIS15, 13, 9, and 7. The data also suggest that high ion and nutrient concentrations in the lake water promote calcite precipitation and diatom growth in the epilimnion during MIS15, 13, and 5, whereas less evaporated interglacial periods exhibit lower TIC and bSi contents (MIS9 and 7).

The most severe glacial conditions at Lake Ohrid occurred during MIS16, 12, 10, and 6, whereas somewhat warmer temperatures can be inferred for MIS14, 8, 4, and 2. Interglacial-like conditions occurred during parts of MIS14 and 8, respectively.

The Supplement related to this article is available online at doi:10.5194/bg-13-1179-2016-supplement.

References

Aliaj, S., Baldassarre, G., and Shkupi, D.: Quaternary subsidence zones in Albania: some case studies, B. Eng. Geol. Environ., 59, 313–318, doi:10.1007/s100640000063, 2001.

Arnaud, F., Revel, M., Chapron, E., Desmet, M., and Tribovillard, N.: 7200 years of Rhone river flooding activity in Lake Le Bourget, France: a high-resolution sediment record of NW Alps hydrology, The Holocene, 15, 420–428, doi:10.1191/0959683605hl801rp, 2005.

Barker, S., Knorr, G., Edwards, R. L., Parrenin, F., Putnam, A. E., Skinner, L. C., Wolff, E., and Ziegler, M.: 800,000 Years of Abrupt Climate Variability, Science, 334, 347–351, doi:10.1126/science.1203580, 2011.

Bar-Matthews, M. and Ayalon, A.: Speleothems as palaeoclimate indicators, a case study from Soreq Cave located in the Eastern Mediterranean Region, Israel, in: Past climate variability through Europe and Africa, edited by: Batterbee, R., Gasse, F., and Stickley, C., Springer, Dordrecht, 363–392, 2004.

Baumgarten, H., Wonik, T., Tanner, D. C., Francke, A., Wagner, B., Zanchetta, G., Sulpizio, R., Giaccio, B., and Nomade, S.: Age-depth model of the past 630 kyr for Lake Ohrid (FYROM/Albania) based on cyclostratigraphic analysis of downhole gamma ray data, Biogeosciences, 12, 7453–7465, doi:10.5194/bg-12-7453-2015, 2015.

Belmecheri, S., Namiotko, T., Robert, C., von Grafenstein, U., and Danielopol, D. L.: Climate controlled ostracod preservation in Lake Ohrid (Albania, Macedonia), Palaeogeogr. Palaeocl., 277, 236–245, doi:10.1016/j.palaeo.2009.04.013, 2009.

Berger, A., Guiot, J., Kukla, G., and Pestiaux, P.: Long-term variations of monthly insolation as related to climatic changes, Geol. Rundsch., 70, 748–758, doi:10.1007/BF01822148, 1981.

Berner, R. A.: A new geochemical classification of sedimentary environments, J. Sediment. Petrol., 51, 359–365, 1981.

Blaauw, M. and Christen, J. A.: Flexible paleoclimate age-depth models using an autoregressive gamma process, Bayesian Analysis, 6, 457–474, doi:10.1214/ba/1339616472, 2011.

Blott, S. J. and Pye, K.: GRADISTAT: A grain size distribution and statistics package for the analysis of unconsolidated sediments, Earth Surf. Proc. Land., 26, 1237–1248, doi:10.1002/esp.261, 2001.

Chen, J., An, Z., and Head, J.: Variation of Rb/Sr Ratios in the Loess-Paleosol Sequences of Central China during the Last 130,000 Years and Their Implications for Monsoon Paleoclimatology, Quaternary Res., 51, 215–219, doi:10.1006/qres.1999.2038, 1999.

Cohen, H.: Paleolimnology: The History and Evolution of Lake Systems, Oxford University Press, New York, 2003.

D'Addabbo, M., Sulpizio, R., Guidi, M., Capitani, G., Mantecca, P., and Zanchetta, G.: Ash leachates from some recent eruptions of Mount Etna (Italy) and Popocatépetl (Mexico) volcanoes and their impact on amphibian living freshwater organisms, Biogeosciences, 12, 7087–7106, doi:10.5194/bg-12-7087-2015, 2015.

Dosseto, A., Hesse, P. P., Maher, K., Fryirs, K., and Turner, S.: Climatic and vegetation control on sediment dynamics during the last glacial cycle, Geology, 38, 395–398, doi:10.1130/g30708.1, 2010.

EPICA-members: Eight glacial cycles from an Antarctic ice core, Nature, 429, 623–628, doi:10.1038/nature02599, 2004.

Fletcher, W. J., Müller, U. C., Koutsodendris, A., Christanis, K., and Pross, J.: A centennial-scale record of vegetation and climate variability from 312 to 240 ka (Marine Isotope Stages 9c–a, 8 and 7e) from Tenaghi Philippon, NE Greece, Quaternary Sci. Rev., 78, 108–125, doi:10.1016/j.quascirev.2013.08.005, 2013.

Föller, K., Stelbrink, B., Hauffe, T., Albrecht, C., and Wilke, T.: Constant diversification rates of endemic gastropods in ancient Lake Ohrid: ecosystem resilience likely buffers environmental fluctuations, Biogeosciences, 12, 7209–7222, doi:10.5194/bg-12-7209-2015, 2015.

Francke, A., Wagner, B., Leng, M. J., and Rethemeyer, J.: A Late Glacial to Holocene record of environmental change from Lake Dojran (Macedonia, Greece), Clim. Past, 9, 481–498, doi:10.5194/cp-9-481-2013, 2013.

Girardclos, S., Schmidt, O. T., Sturm, M., Ariztegui, D., Pugin, A., and Anselmetti, F. S.: The 1996 AD delta collapse and large turbidite in Lake Brienz, Mar. Geol., 241, 137–154, doi:10.1016/j.margeo.2007.03.011, 2007.

Grant, K. M., Rohling, E. J., Bar-Matthews, M., Ayalon, A., Medina-Elizalde, M., Ramsey, C. B., Satow, C., and Roberts, A. P.: Rapid coupling between ice volume and polar temperature over the past 150,000 years, Nature, 491, 744–747, doi:10.1038/nature11593, 2012.

Hoffmann, N., Reicherter, K., Fernández-Steeger, T., and Grützner, C.: Evolution of ancient Lake Ohrid: a tectonic perspective, Biogeosciences, 7, 3377–3386, doi:10.5194/bg-7-3377-2010, 2010.

Holmer, M. and Storkholm, P.: Sulphate reduction and sulphur cycling in lake sediments: a review, Freshwater Biol., 46, 431–451, doi:10.1046/j.1365-2427.2001.00687.x, 2001.

Holtvoeth, J., Rushworth, D., Copsey, H., Imeri, A., Cara, M., Vogel, H., Wagner, T., and Wolff, G. A.: Improved end-member characterisation of modern organic matter pools in the Ohrid Basin (Albania, Macedonia) and evaluation of new palaeoenvironmental proxies, Biogeosciences, 13, 795–816, doi:10.5194/bg-13-795-2016, 2016.

Jovanovska, E., Cvetkoska, A., Hauffe, T., Levkov, Z., Wagner, B., Sulpizio, R., Francke, A., Albrecht, C., and Wilke, T.: Differential resilience of ancient sister lakes Ohrid and Prespa to environmental disturbances during the Late Pleistocene, Biogeosciences Discuss., 12, 16049–16079, doi:10.5194/bgd-12-16049-2015, 2015.

Juschus, O., Melles, M., Gebhardt, A. C., and Niessen, F.: Late Quaternary mass movement events in Lake El'gygytgyn, North-eastern Siberia, Sedimentology, 56, 2155–2174, doi:10.1111/j.1365-3091.2009.01074.x, 2009.

Just, J., Nowaczyk, N., Francke, A., Sagnotti, L., and Wagner, B.: Climatic control on the occurrence of high-coercivity magnetic minerals and preservation of greigite in a 640 ka sediment sequence from Lake Ohrid (Balkans), Biogeosciences Discuss., 12, 14215–14243, doi:10.5194/bgd-12-14215-2015, 2015.

Lacey, J. H., Francke, A., Leng, M. J., Vane, C. H., and Wagner, B.: A high-resolution Late Glacial to Holocene record of environmental change in the Mediterranean from Lake Ohrid (Macedonia/Albania), Int. J. Earth Sci., 104, 1623–1638, doi:10.1007/s00531-014-1033-6, 2015a.

Lacey, J. H., Leng, M. J., Francke, A., Sloane, H. J., Milodowski, A., Vogel, H., Baumgarten, H., and Wagner, B.: Mediterranean climate since the Middle Pleistocene: a 640 ka stable isotope record from Lake Ohrid (Albania/Macedonia), Biogeosciences

Discuss., 12, 13427–13481, doi:10.5194/bgd-12-13427-2015, 2015b.

Lang, N. and Wolff, E. W.: Interglacial and glacial variability from the last 800 ka in marine, ice and terrestrial archives, Clim. Past, 7, 361–380, doi:10.5194/cp-7-361-2011, 2011.

Leicher, N., Zanchetta, G., Sulpizio, R., Giaccio, B., Wagner, B., Nomade, S., Francke, A., and Del Carlo, P.: First tephrostratigraphic results of the DEEP site record from Lake Ohrid, Macedonia, Biogeosciences Discuss., 12, 15411–15460, doi:10.5194/bgd-12-15411-2015, 2015.

Leng, M. J., Roberts, N., Reed, J. M., and Sloane, H. J.: Late Quaternary palaeohydrology of the Konya Basin, Turkey, based on isotope studies of modern hydrology and lacustrine carbonates, J. Paleolimnol., 22, 187–204, doi:10.1023/a:1008024127346, 1999.

Leng, M. J., Baneschi, I., Zanchetta, G., Jex, C. N., Wagner, B., and Vogel, H.: Late Quaternary palaeoenvironmental reconstruction from Lakes Ohrid and Prespa (Macedonia/Albania border) using stable isotopes, Biogeosciences, 7, 3109–3122, doi:10.5194/bg-7-3109-2010, 2010.

Leng, M. J., Wagner, B., Boehm, A., Panagiotopoulos, K., Vane, C. H., Snelling, A., Haidon, C., Woodley, E., Vogel, H., Zanchetta, G., and Baneschi, I.: Understanding past climatic and hydrological variability in the Mediterranean from Lake Prespa sediment isotope and geochemical record over the Last Glacial cycle, Quaternary Sci. Rev., 66, 123–136, doi:10.1016/j.quascirev.2012.07.015, 2013.

Lindhorst, K., Vogel, H., Krastel, S., Wagner, B., Hilgers, A., Zander, A., Schwenk, T., Wessels, M., and Daut, G.: Stratigraphic analysis of lake level fluctuations in Lake Ohrid: an integration of high resolution hydro-acoustic data and sediment cores, Biogeosciences, 7, 3531–3548, doi:10.5194/bg-7-3531-2010, 2010.

Lindhorst, K., Gruen, M., Krastel, S., and Schwenk, T.: Hydroacoustic Analysis of Mass Wasting Deposits in Lake Ohrid (FYR Macedonia/Albania), in: Submarine Mass Movements and Their Consequences, edited by: Yamada, Y., Kawamura, K., Ikehara, K., Ogawa, Y., Urgeles, R., Mosher, D., Chaytor, J., and Strasser, M., Springer, the Netherlands, 245–253, 2012.

Lindhorst, K., Krastel, S., Reicherter, K., Stipp, M., Wagner, B., and Schwenk, T.: Sedimentary and tectonic evolution of Lake Ohrid (Macedonia/Albania), Basin Res., 27, 84–101, doi:10.1111/bre.12063, 2015.

Lisiecki, L. E. and Raymo, M. E.: A Pliocene-Pleistocene stack of 57 globally distributed benthic δ^{18}O records, Paleoceanography, 20, PA1003, doi:10.1029/2004pa001071, 2005.

Magri, D. and Tzedakis, P. C.: Orbital signatures and long-term vegetation patterns in the Mediterranean, Quaternary Int., 73–74, 69–78, doi:10.1016/S1040-6182(00)00065-3, 2000.

Matter, M., Anselmetti, F. S., Jordanoska, B., Wagner, B., Wessels, M., and Wüest, A.: Carbonate sedimentation and effects of eutrophication observed at the Kališta subaquatic springs in Lake Ohrid (Macedonia), Biogeosciences, 7, 3755–3767, doi:10.5194/bg-7-3755-2010, 2010.

Matzinger, A., Jordanoski, M., Veljanoska-Sarafiloska, E., Sturm, M., Müller, B., and Wüest, A.: Is Lake Prespa Jeopardizing the Ecosystem of Ancient Lake Ohrid?, Hydrobiologia, 553, 89–109, doi:10.1007/s10750-005-6427-9, 2006a.

Matzinger, A., Spirkovski, Z., Patceva, S., and Wüest, A.: Sensitivity of Ancient Lake Ohrid to Local Anthropogenic Impacts and Global Warming, J. Great Lakes Res., 32, 158–179, doi:10.3394/0380-1330(2006)32[158:SOALOT]2.0.CO;2, 2006b.

Matzinger, A., Schmid, M., Veljanoska-Sarafiloska, E., Patceva, S., Guseska, D., Wagner, B., Müller, B., Sturm, M., and Wüest, A.: Eutrophication of ancient Lake Ohrid: Global warming amplifies detrimental effects of increased nutrient inputs, Limnol. Oceanogr., 52, 338–353, 2007.

Melles, M., Brigham-Grette, J., Minyuk, P., Nowaczyk, N., Wennrich, V., Deconto, R., Andersen, P., Andreev, A. A., Coletti, A., Cook, T., Haltia-Hovi, E., Kukkonen, M., Lozhkin, A., Rosén, P., Tarasov, P., Vogel, H., and Wagner, B.: 2.8 Million Years of Arctic Climate Change from Lake El'gygytgyn, NE Russia, Science, 337, 315–320, doi:10.1126/science.1222135, 2012.

Meyer-Jacob, C., Vogel, H., Boxberg, F., Rosén, P., Weber, M., and Bindler, R.: Independent measurement of biogenic silica in sediments by FTIR spectroscopy and PLS regression, J. Paleolimnol., 52, 245–255, doi:10.1007/s10933-014-9791-5, 2014.

Meyers, P. A. and Ishiwatari, R.: Organic matter accumulation records in lake sediments, in: Physics and Chemistry of Lakes, edited by: Lerman, A., Imboden, D. M., and Gat, J. R., pringereVerlag Berlin, Heidelberg, New York, 279–328, 1995.

Mohrig, D., Ellis, C., Parker, G., Whipple, K. X., and Hondzo, M.: Hydroplaning of subaqueous debris flows, Geol. Soc. Am. Bull., 110, 387–394, doi:10.1130/0016-7606(1998)110<0387:HOSDF>2.3.CO;2, 1998.

Mulder, T. and Alexander, J.: The physical character of subaqueous sedimentary density flows and their deposits, Sedimentology, 48, 269–299, doi:10.1046/j.1365-3091.2001.00360.x, 2001.

Müller, A.: Late- and Postglacial Sea-Level Change and Paleoenvironments in the Oder Estuary, Southern Baltic Sea, Quaternary Res., 55, 86–96, doi:10.1006/qres.2000.2189, 2001.

Müller, B., Wang, Y., and Wehrli, B.: Cycling of calcite in hard water lakes of different trophic states, Limnol. Oceanogr., 51, 1678–1688, doi:10.4319/lo.2006.51.4.1678, 2006.

NGRIP-members: High-resolution record of Northern Hemisphere climate extending into the last interglacial period, Nature, 431, 147–151, doi:10.1038/nature02805, 2004.

Prokopenko, A. A., Hinnov, L. A., Williams, D. F., and Kuzmin, M. I.: Orbital forcing of continental climate during the Pleistocene: a complete astronomically tuned climatic record from Lake Baikal, SE Siberia, Quaternary Sci. Rev., 25, 3431–3457, doi:10.1016/j.quascirev.2006.10.002, 2006.

Pross, J., Koutsodendris, A., Christanis, K., Fischer, T., Fletcher, W. J., Hardiman, M., Kalaitzidis, S., Knipping, M., Kotthoff, U., Milner, A. M., Müller, U. C., Schmiedl, G., Siavalas, G., Tzedakis, P. C., and Wulf, S.: The 1.35-Ma-long terrestrial climate archive of Tenaghi Philippon, northeastern Greece: Evolution, exploration, and perspectives for future research, Newsl. Stratigr., 48, 253–276, doi:10.1127/nos/2015/0063, 2015.

Reicherter, K., Hoffmann, N., Lindhorst, K., Krastel, S., Fernandez-Steeger, T., Grützner, C., and Wiatr, T.: Active basins and neotectonics: morphotectonics of the Lake Ohrid Basin (FYROM and Albania), Z. Dtsch. Ges. Geowiss., 162, 217–234, doi:10.1127/1860-1804/2011/0162-0217, 2011.

Ribolini, A., Isola, I., Zanchetta, G., Bini, M., and Sulpizio, R.: Glacial feature on the Galicica Mountains, Macedonia: preliminary report, Geogr. Fis. Din. Quat., 34, 247–255, doi:10.4461/GFDQ.2011.34.22, 2011.

Sadori, L., Koutsodendris, A., Masi, A., Bertini, A., Combourieu-Nebout, N., Francke, A., Kouli, K., Joannin, S., Mercuri, A. M., Panagiotopoulos, K., Peyron, O., Torri, P., Wagner, B., Zanchetta, G., and Donders, T. H.: Pollen-based paleoenvironmental and paleoclimatic change at Lake Ohrid (SE Europe) during the past 500 ka, Biogeosciences Discuss., 12, 15461–15493, doi:10.5194/bgd-12-15461-2015, 2015.

Sauerbrey, M. A., Juschus, O., Gebhardt, A. C., Wennrich, V., Nowaczyk, N. R., and Melles, M.: Mass movement deposits in the 3.6 Ma sediment record of Lake El'gygytgyn, Far East Russian Arctic, Clim. Past, 9, 1949–1967, doi:10.5194/cp-9-1949-2013, 2013.

Schnellmann, M., Anselmetti, F. S., Giardini, D., and McKenzie, J. A.: Mass movement-induced fold-and-thrust belt structures in unconsolidated sediments in Lake Lucerne (Switzerland), Sedimentology, 52, 271–289, doi:10.1111/j.1365-3091.2004.00694.x, 2005.

Schnellmann, M., Anselmetti, F., Giardini, D., and McKenzie, J.: 15,000 Years of mass-movement history in Lake Lucerne: Implications for seismic and tsunami hazards, Eclogae Geol. Helv., 99, 409–428, doi:10.1007/s00015-006-1196-7, 2006.

Stein, M., Ben-Avraham, Z., Goldstein, S., Agnon, A., Ariztegui, D., Brauer, A., Haug, G., Ito, E., and Yasuda, Y.: Deep Drilling at the Dead Sea, Sci. Dril., 11, 46–47, doi:10.5194/sd-11-46-2011, 2011.

Stockhecke, M., Kwiecien, O., Vigliotti, L., Anselmetti, F. S., Beer, J., Çağatay, M. N., Channell, J. E. T., Kipfer, R., Lachner, J., Litt, T., Pickarski, N., and Sturm, M.: Chronostratigraphy of the 600,000 year old continental record of Lake Van (Turkey), Quaternary Sci. Rev., 104, 8–17, doi:10.1016/j.quascirev.2014.04.008, 2014a.

Stockhecke, M., Sturm, M., Brunner, I., Schmincke, H.-U., Sumita, M., Kipfer, R., Cukur, D., Kwiecien, O., and Anselmetti, F. S.: Sedimentary evolution and environmental history of Lake Van (Turkey) over the past 600 000 years, Sedimentology, 61, 1830–1861, doi:10.1111/sed.12118, 2014b.

Tzedakis, P. C., McManus, J. F., Hooghiemstra, H., Oppo, D. W., and Wijmstra, T. A.: Comparison of changes in vegetation in northeast Greece with records of climate variability on orbital and suborbital frequencies over the last 450 000 years, Earth Planet. Sci. Lett., 212, 197–212, doi:10.1016/S0012-821X(03)00233-4, 2003.

Tzedakis, P. C., Hooghiemstra, H., and Pälike, H.: The last 1.35 million years at Tenaghi Philippon: revised chronostratigraphy and long-term vegetation trends, Quaternary Sci. Rev., 25, 3416–3430, doi:10.1016/j.quascirev.2006.09.002, 2006.

Urban, N. R., Ernst, K., and Bernasconi, S.: Addition of sulfur to organic matter during early diagenesis of lake sediments, Geochim. Cosmochim. Ac., 63, 837–853, doi:10.1016/s0016-7037(98)00306-8, 1999.

Vogel, H., Wagner, B., Zanchetta, G., Sulpizio, R., and Rosén, P.: A paleoclimate record with tephrochronological age control for the last glacial-interglacial cycle from Lake Ohrid, Albania and Macedonia, J. Paleolimnol., 44, 295–310, doi:10.1007/s10933-009-9404-x, 2010a.

Vogel, H., Wessels, M., Albrecht, C., Stich, H.-B., and Wagner, B.: Spatial variability of recent sedimentation in Lake Ohrid (Albania/Macedonia), Biogeosciences, 7, 3333–3342, doi:10.5194/bg-7-3333-2010, 2010b.

Wagner, B., Reicherter, K., Daut, G., Wessels, M., Matzinger, A., Schwalb, A., Spirkovski, Z., and Sanxhaku, M.: The potential of Lake Ohrid for long-term palaeoenvironmental reconstructions, Palaeogeogr. Palaeocl., 259, 341–356, doi:10.1016/j.palaeo.2007.10.015, 2008.

Wagner, B., Lotter, A. F., Nowaczyk, N., Reed, J. M., Schwalb, A., Sulpizio, R., Valsecchi, V., Wessels, M., and Zanchetta, G.: A 40,000-year record of environmental change from ancient Lake Ohrid (Albania and Macedonia), J. Paleolimnol., 41, 407–430, doi:10.1007/s10933-008-9234-2, 2009.

Wagner, B., Vogel, H., Zanchetta, G., and Sulpizio, R.: Environmental change within the Balkan region during the past ca. 50 ka recorded in the sediments from lakes Prespa and Ohrid, Biogeosciences, 7, 3187–3198, doi:10.5194/bg-7-3187-2010, 2010.

Wagner, B., Francke, A., Sulpizio, R., Zanchetta, G., Lindhorst, K., Krastel, S., Vogel, H., Rethemeyer, J., Daut, G., Grazhdani, A., Lushaj, B., and Trajanovski, S.: Possible earthquake trigger for 6th century mass wasting deposit at Lake Ohrid (Macedonia/Albania), Clim. Past, 8, 2069–2078, doi:10.5194/cp-8-2069-2012, 2012.

Wagner, B., Wilke, T., Krastel, S., Zanchetta, G., Sulpizio, R., Reicherter, K., Leng, M. J., Grazhdani, A., Trajanovski, S., Francke, A., Lindhorst, K., Levkov, Z., Cvetkoska, A., Reed, J. M., Zhang, X., Lacey, J. H., Wonik, T., Baumgarten, H., and Vogel, H.: The SCOPSCO drilling project recovers more than 1.2 million years of history from Lake Ohrid, Sci. Dril., 17, 19–29, doi:10.5194/sd-17-19-2014, 2014.

Wang, Y., Cheng, H., Edwards, R. L., Kong, X., Shao, X., Chen, S., Wu, J., Jiang, X., Wang, X., and An, Z.: Millennial- and orbital-scale changes in the East Asian monsoon over the past 224,000 years, Nature, 451, 1090–1093, doi:10.1038/nature06692, 2008.

Watzin, M., Puka, V., and Naumoski, T.: Lake Ohrid and its Watershed. State of the Environment Report, Lake Ohrid Conservation Project, Tirana, Albania and Ohrid, Macedonia, 2002.

Wennrich, V., Minyuk, P. S., Borkhodoev, V., Francke, A., Ritter, B., Nowaczyk, N. R., Sauerbrey, M. A., Brigham-Grette, J., and Melles, M.: Pliocene to Pleistocene climate and environmental history of Lake El'gygytgyn, Far East Russian Arctic, based on high-resolution inorganic geochemistry data, Clim. Past, 10, 1381–1399, doi:10.5194/cp-10-1381-2014, 2014.

Wick, L., Lemcke, G., and Sturm, M.: Evidence of Lateglacial and Holocene climatic change and human impact in eastern Anatolia: high-resolution pollen, charcoal, isotopic and geochemical records from the laminated sediments of Lake Van, Turkey, The Holocene, 13, 665–675, 10.1191/0959683603hl653rp, 2003.

Wold, S., Sjöström, M., and Eriksson, L.: PLS-regression: a basic tool of chemometrics, Chemometr. Intell. Lab., 58, 109–130, doi:10.1016/S0169-7439(01)00155-1, 2001.

Zanchetta, G., Regattieri, E., Giaccio, B., Wagner, B., Sulpizio, R., Francke, A., Vogel, L. H., Sadori, L., Masi, A., Sinopoli, G., Lacey, J. H., Leng, M. L., and Leicher, N.: Aligning MIS5 proxy records from Lake Ohrid (FYROM) with independently dated Mediterranean archives: implications for core chronology, Biogeosciences Discuss., 12, 16979–17007, doi:10.5194/bgd-12-16979-2015, 2015.